Preparation of tris(azolyl)phosphine gold(I) complexes: digold(I) coordination and variation in solid state intermolecular interactions†

Christoph E. Strasser, William F. Gabrielli, Catharine Esterhuysen, Oliver B. Schuster, Stefan D. Nogai, Stephanie Cronje and Helgard G. Raubenheimer*

Received (in Durham, UK) 6th July 2007, Accepted 30th August 2007
First published as an Advance Article on the web 14th September 2007
DOI: 10.1039/b709896k

Various tris(azolyl)phosphines R_3P (R = 1-methylimidazol-2-yl, thiazol-2-yl, 4-methylthiazol-2-yl or 4,5-dimethylthiazol-2-yl) (**1a–d**) were utilised to prepare complexes of the type R_3PAuCl (**2a–d**). The donor strength of the nitrogen atoms was assessed with natural-abundance $^{15}N\{^1H\}$ NMR of **1a–c** and **2a–c**. The chloride of **2c** could be successfully substituted by the anions BzS^- and NCS^-. Further utilisation of the imine nitrogens of the tris(azole)phosphines to coordinate additional Au^I centres was successful only for **2a** where treatment with 3 mole equivalents of $C_6F_5Au(tht)$ (tht = tetrahydrothiophene) afforded bis(pentafluorophenyl)-μ-[tris(1-methylimidazol-2-yl)phosphine-κ^2P,N]digold(I) (**4**). A hydrolysis product consisting of two bis(1-methylimidazol-2-yl)phosphinite ligands bridging a Au_2^{4+} centre and further coordination to two AuC_6F_5 moieties (**5**) was formed during this reaction. The crystal and molecular structures were determined of compounds **1d**, **2a–d** and **3b**. Intriguingly, **2b** and **2c** crystallise in a total of seven polymorphs and solvates exhibiting different modes of intermolecular association. Compound **2b** crystallises in three polymorphs; two of them and the solvate **2b** · $0.5CH_2Cl_2$ exhibit aurophilic interaction while the third one is stabilised by a short Au···Cl interaction of 3.2660(9) Å. In **2c**, one polymorph exhibits a strong aurophilic interaction of 3.0393(4) Å, but the other, as well as the solvate **2c** · thf, lack such contacts. Product **2b** is the first simple gold compound known to have both Au···Au or Au···Cl contacts in different crystals. Calculations at the B3LYP and MP2 levels of theory using quasi-relativistic basis sets show that for $\mathbf{2b}_2$ the Au···Cl interaction is between 2.6 and 12.2 kJ mol^{-1} greater than the Au···Au interaction, depending on the level of theory and basis set. This contrasts with a model $(PH_3AuCl)_2$ dimer, where the Au···Au interaction is found to be stronger.

Introduction

Alkyl- and arylphosphines count amongst the most useful ligands in coordination chemistry. However, complexes of phosphines with one or more azolyl residues have received much less attention. The literature available deals mainly with complexes of (1-alkylimidazol-2-yl)diphenylphosphines where cationic, bridged, dinuclear coinage metal complexes with P,N-coordination of the metals are a popular motif.[1] A mixed Ag^I/Au^I complex has been reported in which the gold centre is selectively coordinated by the phosphorus atoms and the silver centre solely by the imidazole nitrogen atoms.[2]

Metal complexes of tris(imidazolyl)phosphine ligands are mainly used as molecular models for carbonic anhydrase.[3] In these instances only the imine nitrogen atoms are utilised as coordination centres resembling the κ^3N-coordination mode found in similar complexes of the hydridotris(pyrazol-2-yl)-borate scorpionate ligands, the phosphorus serving mainly as a probe for convenient ^{31}P NMR analysis. Employment of tris(imidazolyl)phosphines as P-coordinating ligands has only been reported in two instances for Au^I and Pt^{II} complexes,[4] the former being the only P-coordinated tris(azolyl)phosphine complex so far characterised by X-ray diffraction.

Examples of complexes of phosphines with thiazolyl moieties are even less common and for the Au^I centre only diphenyl(thiazol-2-yl)phosphine[5] and, recently, a fluorinated (benzothiazol-2-yl)diphenylphosphine[6] have been employed. Other examples that were found to exhibit N-coordination of one (benzo)thiazole moiety in addition to phosphine coordination, include complexes of Rh^I and Rh^{II},[7] and Fe^0/Cd^{II} and Fe^0/Hg^{II},[8] which have been characterised by X-ray crystal structure determinations. Tris(thiazolyl)phosphine, in turn, has only found applications in two reports of Rh^I and Pt^{II} complexes,[4a,9] albeit no crystal and molecular structures of complexes with this ligand have been determined.

Prompted by the scarcity of tris(azolyl)phosphine complexes, we set out to explore the coordination chemistry of these ligands towards the Au^I centre and obtain structural information for the new complexes formed. The chemical reactivity of these compounds as well as their ability to act as ligands themselves was probed. Unexpectedly, Au^I complexes of tris(azolyl)phosphines were susceptible to hydrolysis

Department of Chemistry and Polymer Science, University of Stellenbosch, Private Bag X1, Matieland, 7602, South Africa. E-mail: hgr@sun.ac.za; Fax: +27 21 808 3849; Tel: +27 21 808 3850
† Electronic Supplementary Information (ESI) available: Colour figures for all crystal structures reported. See http://dx.doi.org/10.1039/b709896k/

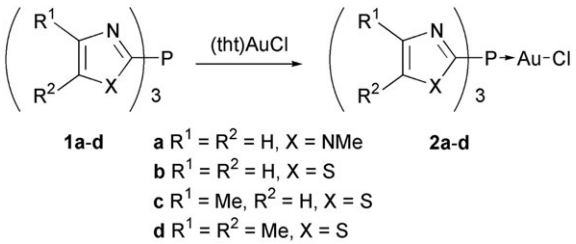

Scheme 1

of one azolyl moiety, a reaction only observed before for Os^{II} complexes—and there in an intramolecular manner with simultaneous migration of one phenyl group.[10] Some ligands and complexes were now also examined by natural abundance $^{15}N\{^1H\}$ NMR spectroscopy constituting, to our knowledge, the first such study of heterocyclic phosphines.

Results and discussion

The ligands were prepared according to literature protocol,[4a] except for the preparation of the very hydrophilic **1a**, where the workup required repeated extraction of the aqueous layer with dichloromethane instead of the reported diethyl ether, and for **1d**, requiring a reaction temperature of −78 °C.

Synthesis of the gold complexes **2a–d** (Scheme 1) was effected by substitution of tht in (tht)AuCl in dichloromethane solution. The resulting compounds are generally soluble in polar aprotic solvents such as thf and dichloromethane but **2a** is somewhat less soluble in these solvents although well soluble in methanol. The products are thermally stable and can be stored at room temperature for prolonged periods of time without noticeable decomposition.

Attempts to substitute the chloride in **2c** by using aqueous NaNCS in a biphasic reaction[11] or by treatment with RSLi (R = $CH_2C_6H_5$, C_6H_5 or C_6H_5CO) in anhydrous thf produced only the two complexes **3a** and **3b** that contain electron-withdrawing residues attached to the sulfur (Scheme 2). With phenylmethanethiolate and benzenethiolate precipitation of $(AuSR)_n$ and liberation of the free phosphine was observed. The electronic nature of tris(thiazol-2-yl)phosphinegold(I) chlorides thus differs greatly from triphenylphosphinegold(I) chloride ($Ph_3PAuSPh$ is readily available)[12] and is comparable

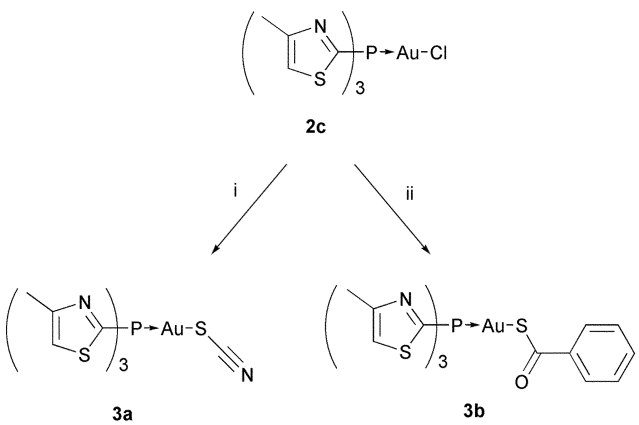

Scheme 2 *Reagents and conditions*: (i) aqueous NaNCS/dichloromethane; (ii) BzSLi in anhydrous thf.

to that of chlorotris[3,5-bis(trifluoromethyl)phenyl]phosphinegold(I). Employment of this compound and substitution of the chloride with benzenethiolate, gave the product in only 6% yield due to fast decomposition in solution.[13]

Reaction of **2c** with $NaCH(CN)_2$ in anhydrous thf yielded a mixture; a reaction occurred according to the $^{31}P\{^1H\}$ NMR spectrum but again attempts to isolate a pure product failed. Compounds **3a** and **3b** are somewhat less stable than **2a–d** at room temperature and slow decomposition with deposition of metallic gold occurs.

Subsequently, the possibility of the imine nitrogens acting as additional coordination centres towards gold was explored. In reactions between the new phosphine complexes and $C_6F_5Au(tht)$ a clear discrimination was found in that only **2a**, that contains an imidazolylphosphine ligand, coordinated to another gold centre. Addition of an excess of $C_6F_5Au(tht)$ to **2a** afforded a mixture of products of which two could be isolated. In the major reaction, AuCl was substituted for AuC_6F_5 and only one imidazole nitrogen atom was further coordinated to another AuC_6F_5 group, stabilised by an intramolecular aurophilic interaction (Scheme 3). In an unprecedented fashion, a multinuclear complex with an Au_2^{4+} centre coordinated by two bridging bis(1-methylimidazol-2-yl)phosphinite ligands in which each methylimidazolyl moiety further coordinates to another AuC_6F_5 group, was formed. However, a crystal structure determination which yielded the precise connectivity of the atoms in the compound is not of publishable quality.

Following these results, complex **4** was independently synthesised by reacting ligand **1a** with two mole quantities of $C_6F_5Au(tht)$ to obtain an analytically pure compound (Scheme 3). In the solid form, both the acetone solvate crystals and the solvent-free powder are stable at −16 °C but decompose slowly when dissolved and stored at room temperature.

Investigation of the hydrolytic behaviour of the oxides and alkylphosphonium salts of tris(2-furyl)- and tris(2-thienyl)-phosphine have been shown to effect the corresponding phosphinic acids.[14] The hydrolysis of complex **2a** can thus be rationalised as a special case in which an alkyl cation is formally replaced by $(azolyl)_3PAu^+$. Severance of P–C bonds in tris(imidazolyl)phosphines has been observed previously by other authors in attempts to prepare chloro[tris(4,5-dimethyl-imidazol-2-yl)phosphine]gold(I) leading to the formation of a bis(carbene)gold(I) derivative,[15] and tris(imidazol-2-yl)phosphine which converts into bis(imidazol-2-yl)phosphinic acid.[16] As hydrolysis was not observed during the preparation of **3a** the hydrolysis of tris(thiazolyl)phosphines was further investigated. For this purpose **2c** was dissolved in DMSO-d_6 and one equivalent of aqueous NaOH added. The solution instantly became hot and a colourless precipitate was observed. A $^{31}P\{^1H\}$ NMR spectrum of the product proved the complete consumation of **2c** but again none of the products could be isolated.

As we always observed initial P-coordination of the ligands it is apparent that the coordination chemistry of Au^I to tris(imidazolyl)phosphines is markedly different when compared to the isoelectronic Hg^{II}. A cationic tris(1-isopropyl-4-*tert*-butylimidazol-2-yl)phosphine Hg^{II} complex has been shown to exhibit κ^3N-coordination by the imidazole nitrogens

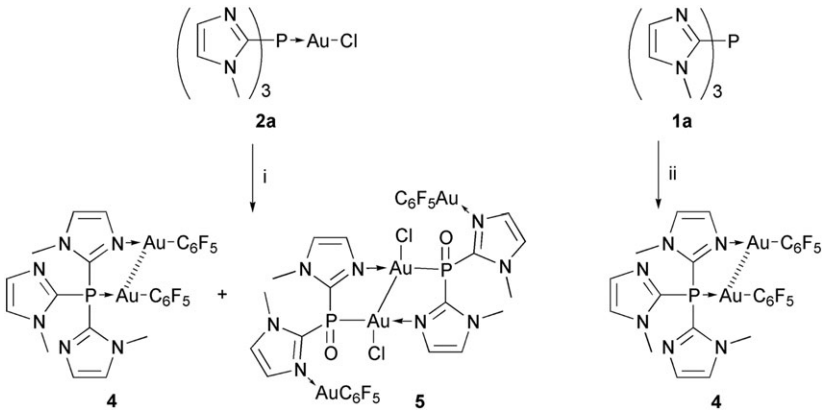

Scheme 3 *Reagents and conditions*: (i) 3 mole equivalents of $C_6F_5Au(tht)$; (ii) 2 mole equivalents $C_6F_5Au(tht)$.

but no coordination to the phosphorus took place.[17] Consequently it appears that with tris(imidazolyl)phosphines, phosphorus is the superior donor atom for Au^I and Pt^{II} but not for other metals examined so far. On the other hand, in the few instances examined, tris(thiazol-2-yl)phosphines have only been found to coordinate through the phosphorus atom and no involvement of the nitrogen atoms was detected.[4a,9] It is anticipated that coordination of tris(thiazol-2-yl)phosphines to hard metal centres could lead to interesting coordination modes.

NMR spectroscopy

All complexes have been investigated by multinuclear NMR spectroscopy including natural-abundance $^{15}N\{^1H\}$ NMR for compounds **1a–c** and **2a–c**. The tris(thiazol-2-yl)phosphine ligands and complexes all furnish expected ^1H, ^{13}C and ^{31}P NMR spectra. In the ^1H NMR spectrum the methyl resonances of **1d** are isochronous, their different nature was only revealed in the ^{13}C NMR spectrum where they are well separated. In complex **2d** the two inequivalent methyl resonances in the ^1H NMR spectrum are just resolved. However, **1a** and **2a** furnish three signals for the C4 carbon atom indicating a rotation barrier for the imidazolyl moieties around the P–C bond which can be attributed to the bulky 1-methyl substituent. However, a similar signal splitting was not observed in the NMR spectra of the even bulkier tris(1-ethenylimidazol-2-yl)phosphine and tris[1-methyl-4-(4-methylphenyl)imidazol-2-yl]phosphine.[18] In the tris(thiazolyl)-phosphine ligands, coupling of the different hydrogens to each other and sometimes to the phosphorus can be resolved and the coupling constants identified by selective irradiation experiments on the respective protons in **2b** and **2c**. J_{HH} and J_{PH} are enhanced by coordination to the Au^I centre; in some instances coordination rendered an additional J_{PH} coupling which was not resolved in the spectrum of the free ligand. Similar observations have been made with other heterocyclic phosphines.[18a,19]

Enhancement of the J_{PC} couplings of the ligand were also noted, especially for the *ipso*-carbon atom; this is in agreement with similar trends in simple arylphosphines but the effect is now more pronounced. The *ipso*-J_{PC} for **2a–d** are seen in the range 90–120 Hz compared to 62.4 Hz in Ph_3PAuCl.[20]

The ^{31}P NMR spectra of **2a–d** show a substantial downfield shift of *ca.* 30 to 40 ppm compared to the free ligands which is generally observed on complexation of tertiary phosphines to Au^I. Possible η^1-κN-coordination of Au^I should give only a slight upfield shift as chelating κ^3N-scorpionate coordination results in strong shielding of the ^{31}P nucleus by 50 ppm for a variety of metals.[19b,21] Still, the phosphorus atom is the softer coordination site and thus is preferred by the soft Au^I centre to the imine nitrogen lone pairs; however tetrahedral coordination of Au^I has been observed with the hydridotris(pyrazolyl)borate ligand class.[22]

^{15}N NMR spectroscopy

The reluctance of the azole nitrogen atoms in tris(azolyl)phosphines to coordinate to Au^I, which contrasts previous results with azoles,[23] motivated us to determine their chemical shifts and thus natural abundance ^1H detected $^1H,^{15}N$ gHMQC spectra of compounds **1a–c** and **2a–c** in order to estimate their donor strength were measured. The ^{15}N NMR spectrum of 4-methylthiazole was determined for comparison by direct detection of the ^{15}N nucleus as an gHMQC experiment failed to yield a signal even at low temperature. The nitrogen nuclei become less shielded in the order free azole $\gg$ tris(azolyl)phosphine $>$ chloro[tris(azolyl)phosphine]gold(I). As expected, nitrogen atoms in the thiazole rings were less shielded than N3 in the imidazole rings. As no N-coordination could be achieved in the instance of the tris(thiazolyl)phosphines, it is estimated that tht coordinated to Au^I is only substituted by the azole nitrogen if the ^{15}N chemical shift occurs upfield from *ca.* δ −60.

As the J_{PC} and J_{PH} coupling constants become larger upon coordination of the ligand, the question arose whether this trend would be reflected also for J_{PN} coupling constants. While complexes **2a–c** all show P–N coupling, this coupling was only clearly resolved in free ligand **1a**. It seems that the coupling is again enhanced by coordination of the phosphorus, yet further examples would be necessary to confirm the trend. Table 1 shows ^{15}N chemical shifts of the free azoles, **1a–c** and **2a–c** and $^3J_{PN}$ coupling constants.

The limited literature available on P–N coupling constants mainly deals with $^1J_{PN}$ values of phosphoramidite and phosphinous amide derivatives and their oxidation products with

Table 1 ^{15}N NMR data for azoles and compounds **1a–c** and **2a–c**

Compound	Solvent	δ_N (ppm) and $[J_{PN}]$/Hz
1-Methylimidazole[25]	$(CD_3)_2SO$	–119.1 (N3), –219.2 (N1)
	$CDCl_3$	–124.1 (N3), –221.7 (N1)
Thiazole	Neat[26]	–57.2
	$CDCl_3$[25]	–62.0
4-Methylthiazole	80% v/v in $CDCl_3$[a]	–52.9
1a	$(CD_3)_2SO$	–97.5 [50 ± 5] (N3), –208.1 (N1)
1b	CD_2Cl_2	–41.3
1c	CD_2Cl_2	–35.4
2a	$(CD_3)_2SO$	–90.6 [89.3] (N3), –206.31 (N1)
2b	CD_2Cl_2	–33.9 [27.8]
2c	CD_2Cl_2	–29.5 [89.4]

[a] Direct detection.

oxygen, sulfur or selenium. In these instances either minor changes or a substantial decrease in the coupling constants is associated with the increase in coordination from tri- to tetracoordinate phosphorus.[21,24]

Crystallography

Most polymorphic crystal and molecular structures of **2b** and **2c** exhibit aurophilic interactions in the solid state while no Au···Au contacts are observed in the structures of **2a**, **2d** and **3b**. This may be due to the steric demand of the phosphine ligands or the thiobenzoate, respectively. The molecular structures of **4** exhibit short aurophilic interactions facilitated by the bridging ligand. Selected bond lengths and angles are summarised in Table 2.

Polymorphs and solvates of 2b and 2c

Three polymorphs, (i) (ii) and (iii), and a hemi-dichloromethane solvate were obtained for **2b**. Two polymorphs of **2c** and a thf solvate were found but only **2c(i)** exhibits a rather short aurophilic interaction, the other crystal structures contain only discrete molecules. Polymorphism in gold compounds focussing on luminescence has been studied previously and was summarised in a review.[27]

Aurophilic interactions in both monoclinic **2b(i)** (space group $P2_1/c$) and triclinic **2b(ii)** ($P\bar{1}$; see Fig. 1) are weak resulting in nearly linear Cl–Au–P angles. The Cl–Au···Au–Cl torsion angle is close to 180° for **2b(i)** and 180° for **2b(ii)** also maximising the dipole interaction between the molecules.[28] Compared to the molecular structure of **2c(i)** these results are surprising considering that the aurophilic interaction is considerably stronger in this structure (*vide infra*) while the ligand is bulkier. Furthermore, in **2b(i)** a close Cl···S contact of 3.373(1) Å between Cl(1) and S(11′) (′ = $x-1, y, z$) linking the molecules along the *a* axis can be observed; the related distance between Cl(2) and S(41″) (″ = $1+x, y, z$) in the other crystallographically independent molecule is much longer [3.389(1) Å].

We attempted to utilise the comparatively weak aurophilic interactions (but with less steric hindrance) of **2b(i)** and **2b(ii)** with the strong interaction of **2c(i)** to crystallise a dimer consisting of both molecules. Needles of a new habit were indeed observed in the Schlenk tube. The molecular structure, however, was that of **2b** · $0.5CH_2Cl_2$. It consists of two crystallographically independent molecules associated by an aurophilic interaction and a close contact of 3.334(3) Å between Cl(2) and S(61′) (′ = $1/2+x, 1/2-y, 1/2+z$). While in every complex of ligands **1b** and **1c** at least one sulfur of the thiazole rings points towards the Au^I centre with typical distances of

Table 2 Selected bond lengths (Å), bond angles (°) and torsion angles (°)

Compound	Au–Cl	Au–P	Au···Au	Au–N	(P)Au–C	(N)Au–C	Cl–Au–P	P–Au–C	N–Au–C	Cl–Au···Au–Cl	P–Au···Au–N
2a	2.276(2)	2.218(1)	—	—	—	—	178.59(5)	—	—	—	—
2b(i)	2.2774(9)	2.2184(9)	3.4563(2)	—	—	—	174.06(4)	—	—	162.52(4)	—
	2.276(1)	2.217(1)					178.03(4)				
2b(ii)	2.2900(9)	2.2260(9)	3.3459(3)	—	—	—	174.30(3)	—	—	180[a]	—
2b(iii)	2.2921(8)	2.2096(8)	—	—	—	—	176.36(3)	—	—	180[a]	—
2b · $0.5CH_2Cl_2$	2.285(2)	2.214(2)	3.2044(5)	—	—	—	168.97(9)	—	—	161.21(9)	—
	2.275(2)	2.212(2)					174.00(9)				
2c(i)	2.2901(8)	2.2169(8)	3.0394(4)	—	—	—	167.83(3)	—	—	74.65(4)	—
2c(ii)	2.283(1)	2.214(1)	—	—	—	—	178.49(4)	—	—	—	—
	2.277(1)	2.211(1)					176.59(4)				
2c · thf	2.271(1)	2.211(1)	—	—	—	—	178.92(6)	—	—	—	—
2d	2.281(1)	2.218(1)	—	—	—	—	179.34(5)	—	—	—	—
3b · $0.5C_6H_{14}$	2.298(2)[b]	2.250(2)	—	—	—	—	174.53(6)[b]	—	—	—	—
4 · Me_2CO	—	2.263(2)	2.9620(5)	2.074(7)	2.029(8)	2.019(8)	—	175.9(2)	178.5(3)	—	20.9(2)
4 · $0.83CDCl_3$	—	2.265(2)	3.0240(4)	2.060(5)	2.047(6)	2.004(6)	—	172.2(2)	178.5(2)	—	23.5(1)
		2.275(2)	3.0170(4)	2.062(5)	2.046(6)	2.003(6)		174.5(2)	173.0(2)		27.1(1)
		2.266(2)	2.9903(4)	2.060(5)	2.045(6)	2.008(6)		170.1(2)	179.0(2)		20.1(1)

[a] Imposed by centre of inversion. [b] Au–S distance and S–Au–P angle.

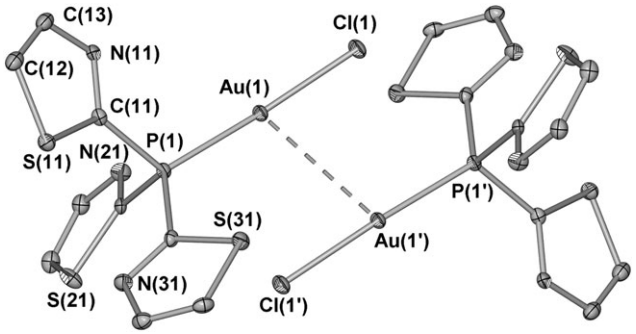

Fig. 1 Molecular structure of compound **2b(ii)**. Thermal ellipsoids are shown at the 50% probability level.

3.57–3.89 Å in what could amount to a weak Au···S interaction, **2b** · $0.5CH_2Cl_2$ is the only structure where a nitrogen atom is positioned in such a manner. Intriguingly, blocks of the already known triclinic **2b(ii)** were found alongside the needles in the same crystallisation vessel.

Later a crystal of the third polymorph **2b(iii)** in the space group $P\bar{1}$ was discovered, originating from the same vessel as **2b** · $0.5CH_2Cl_2$. The molecular structure of **2b(iii)** (Fig. 2) does not exhibit Au···Au interactions like all other structures of **2b** but is instead stabilised by very short intermolecular Au···Cl contacts of 3.2660(9) Å between molecules ordered into dimers (symmetry operator $1 - x, 2 - y, -z$). This mode of stabilisation is observed for other tris-heterocyclic phosphines like chloro[tris(2-furyl)phosphine]gold(I),[29] chloro[tris(2-thienyl)-arsine]gold(I)[30] and fluorinated derivatives of chloro(triphenylphosphine)gold(I).[31] Furthermore a contact of Cl(1) and S(21′) (′ = $1 + x, 1 + y, z$) of 3.472(1) Å is observed. To our knowledge **2b** is the first example of a compound exhibiting both kinds of aggregation in different polymorphs, with **2b(iii)** showing one of the closest intermolecular Au···Cl contact distances known for a neutral Au^I compound. The similar structures of **2b(ii)** and **2b(iii)** allow for direct comparison of the effects of the different associations. Especially the Au–P bond is significantly shortened by the Au···Cl interaction while the Au–Cl bonds are of comparable length. While association *via* halogen bridges is common for Cu^I and Ag^I, *ab initio* calculations suggest that Au^I should prefer metallophilic interaction to other means of aggregation.[28] However, replacement of PH_3 with tris-heterocyclic phosphines might influence this affinity towards the bridging instance.

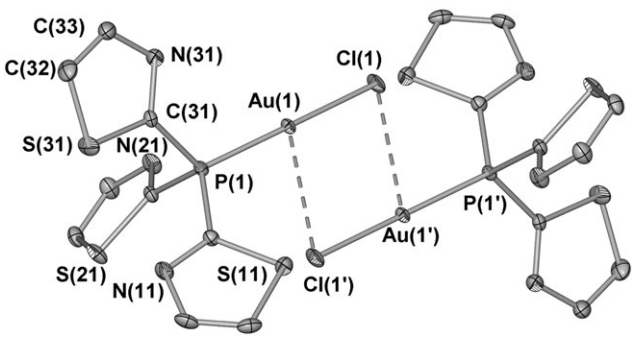

Fig. 2 Molecular structure of compound **2b(iii)**. Thermal ellipsoids are shown at the 50% probability level.

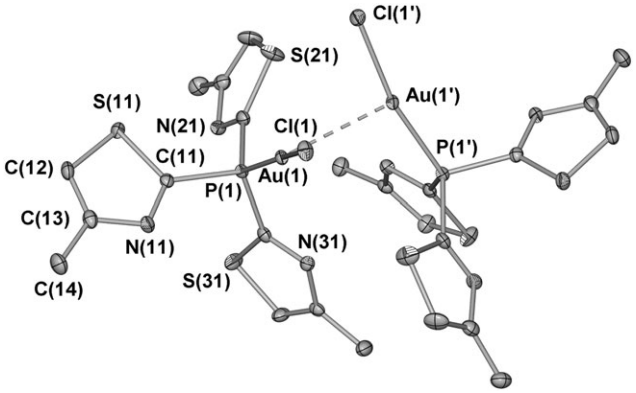

Fig. 3 Molecular structure of compound **2c(i)**. Thermal ellipsoids are shown at the 50% probability level.

Several compounds are known where solvate formation is accompanied by changes in the type or strength of aurophilic interaction.[32] Yet, to our knowledge, only one example is known of a compound crystallised unsolvated and solvated with and without aurophilic interactions.[33] These authors crystallised the $[(MeNH)(MeO)C]_2Au^+$ cation with the anion of 2,3-dichloro-5-cyano-6-hydroxy-*p*-benzoquinone. The molecular structure of the solvent-free salt crystal consists of dimers of the cation held together by an aurophilic interaction of 3.196 Å while crystals of the trichloromethane solvate consist of single cations sandwiched between two anions. The presence of hydrogen bonds in both structures indicates that such bonds play an important role in governing the packing of these structures given that the strength of aurophilic interactions was found to be of similar magnitude.[34]

In the course of our work, three crystal and molecular structures containing **2c** were determined, the first one [**2c(i)**] in the monoclinic space group $C2/c$ obtained by crystallisation of the compound from dichloromethane/diethyl ether wherein the molecules form dimers held together by a strong aurophilic interaction, the strength being reflected in the distortion of the P–Au–Cl angle (Fig. 3). The second one, **2c** · thf, shown in Fig. 4, was obtained by crystallisation of **2c** from thf/pentane. They crystallise in the orthorhombic space group $P2_12_12_1$ and

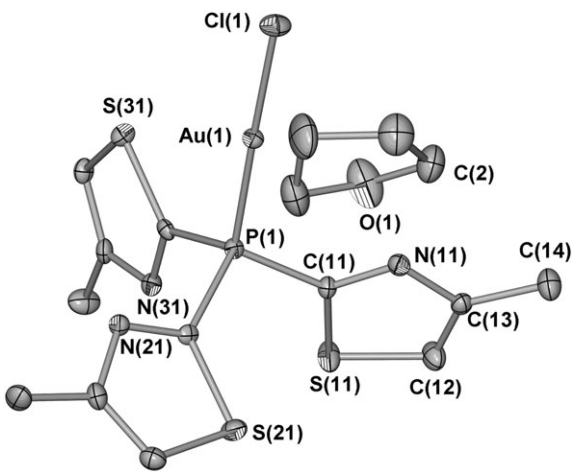

Fig. 4 Molecular structure of compound **2c** · thf. Thermal ellipsoids are shown at the 50% probability level.

consist of discrete molecules packed around channels running parallel to the *b* axis incorporating the thf. The P–Au–Cl angle approaches linearity as is expected for an undisturbed coordination sphere around a Au^{I} centre. Cooperative interaction of **2c** with the thf molecule is sufficiently strong to override the attraction between the Au centres. A contact between Cl(1) and S(21′) [′ = *x*, *y* − 1, *z*; 3.534(2) Å], roughly equal to the sum of the van der Waals radii, is also observed, but longer and weaker than in the structures of **2b**. Without the influence of the aurophilic interaction, the Au–P and especially the Au–Cl bond in **2c** · thf are significantly strengthened as is reflected in their shorter bond lengths than those found in **2c(i)**. A second polymorph, **2c(ii)**, was found alongside crystals of **2c(i)** in another crystallisation from dichloromethane/hexane and was later also isolated amongst **2c** · thf in a repeated crystallisation from thf–pentane. Monoclinic **2c(ii)** crystallises in the space group $P2_1/c$ with two crystallographically independent molecules with similar arrangement of the thiazole moieties. The molecules form crystallographically independent alternating layers parallel to the *ac* plane. To our great surprise, the molecular structure of this polymorph did not exhibit any aurophilic interactions or sub-van der Waals contacts. There are only two other examples of compounds crystallising in polymorphs with and without aurophilic interactions, chlorotris(4-methylphenyl)phosphinegold(I)[35] and μ-(dppm)$(AuCl)_2$ [dppm = bis(diphenylphosphino)methane].[36] The length of the Au–Cl and Au–P bonds is intermediate between those in structure **2b(i)** and the thf solvate. While we believe that crystallisation from dichloromethane will give polymorph **2c(i)** as the major product, the crystals of **2c(ii)** may in fact be quite similar in energy. The structures of **2b(ii)** and **2b(iii)** as well as **2c(i)** and **2c(ii)** constitute concomitant polymorphs[37] by virtue of their simultaneous isolation from the same crystallisation vessels. This raises the question to which extent concentration, temperature and solvent composition influence the crystallisation process, and hence interaction modes, of these compounds.

Crystal and molecular structures of 1d, 2a, 2d, 3b and 4

The molecular structure of **2d** shown in Fig. 5 exhibits a thiazole ring that occupies two different positions that are flipped by 180°. The lack of discrimination between the S- and N-orientations is most likely due to the two methyl substituents at the thiazole given that no disorder was found in structures of ligand **1b**. The lone pair of the thiazole nitrogen atoms may have some directing influence on the conformation of the ring as disorder was observed in complexes of the sterically similar tris(2-thienyl)phosphine.[30] The absolute structure of **2d** in the polar space group $Pna2_1$ could not be established due to the disorder yielding an ambiguous Flack *x* parameter. The packing in the crystals of **1d** in turn allows for such a discrimination and no disorder is observed. The steric bulk of the ligand is just enough to render aurophilic interactions unfavourable and complex **2d** crystallises as discrete molecules. The Au–Cl and Au–P bond lengths are roughly comparable to the values in **2c(ii)** but longer than in **2c** · thf.

The molecular structure of **2a** displayed in Fig. 6 consists of discrete molecules, the absence of Au···Au contacts is probably caused by the steric demand of the ligand. Tris(2-methylphenyl)phosphine has a similar steric requirement to ligand **1a** and greatly inhibits Au···Au contacts even in bridged binuclear complexes.[38] Structures where such contacts are present are all polyaurated onium species.[39] One of the imidazole rings in **2a** is disordered and occupies two positions within the plane of the ring. This disorder may also be present in the structure of **3b** · $0.5C_6H_{14}$ where the direction of the thermal displacement ellipsoids suggest a minute mobility of one thiazole ring in its respective plane, but this could not be resolved.

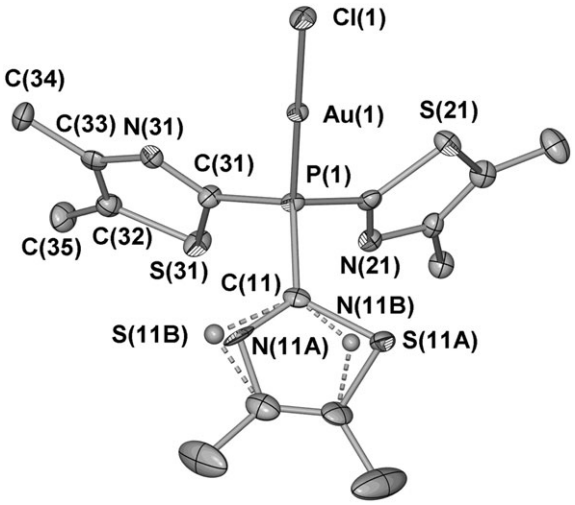

Fig. 5 Molecular structure of compound **2d**. The minor orientation of the thiazole ring containing C(11) is shown as spheres of arbitrary radius. Thermal ellipsoids are shown at the 50% probability level.

The complex **3b** · $0.5C_6H_{14}$ shown in Fig. 7 crystallises in discrete molecules without any Au···Au interactions as a result of the bulky thiobenzoate group. The porous structure consists of alternating layers of the phosphinegold and solvent/thiobenzoate domains along the *c* axis, whereas the

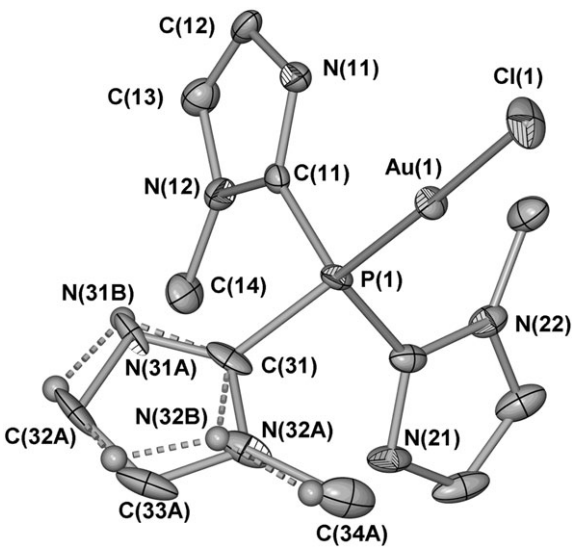

Fig. 6 Molecular structure of compound **2a**. The minor orientation of the imidazole ring containing C(31) is shown as spheres of arbitrary radius. Thermal ellipsoids are shown at the 50% probability level.

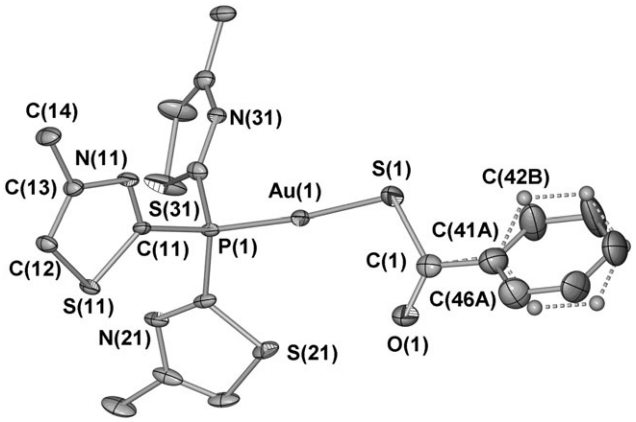

Fig. 7 Molecular structure of compound **3b** · $0.5C_6H_{14}$. The minor orientation of the phenyl ring is shown as spheres of arbitrary radius. Disordered hexane solvent is not shown. Thermal ellipsoids are shown at the 50% probability level.

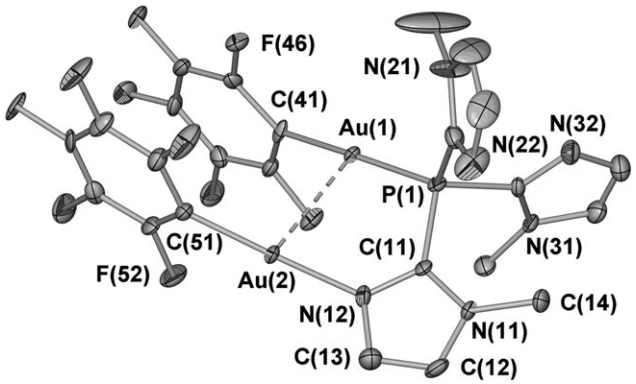

Fig. 8 Molecular structure of compound **4** · Me_2CO. The acetone solvent is omitted for clarity. Thermal ellipsoids are shown at the 50% probability level.

hexane molecules and the thiobenzoate residues are themselves ordered into channels running along the *a* axis. The phenyl ring of the thiobenzoate is disordered into two positions, probably influenced by the highly disordered crystal solvent which could not be modelled.

The structure of the binuclear complex **4** · Me_2CO shown in Fig. 8 is propagated by π-stacking of the C_6F_5 moieties in the *ab* plane. A strong intramolecular aurophilic bond, facilitated by the bridging ligand, is formed between the two gold atoms. The bond lengths are in the range as observed for other imine-coordinated AuC_6F_5 moieties;[23] the Au–P bond however is longer than in **2a** which might result from the strong aurophilic interaction, a similar trend was found in $dppm(AuCl)_2$[36b] and $dppm(AuC_6F_5)_2$ (Au···Au 3.163 Å).[40] The opposite is true for the isolated gold complexes Ph_3PAuCl[41] and $Ph_3PAuC_6F_5$,[42] with the latter compound having the longer Au–P bond. The cocrystallised acetone molecules form channels running along the *a* axis and are readily removed by applying a vacuum to the crystals, resulting in the collapse of the structure. The structure of **4** · $0.83CDCl_3$ shown in Fig. 9 is remarkable in that it consists of three crystallographically independent molecules all showing a comparable arrangement as in the acetone solvate. A notable exception is the N(31)–Au(4) bond vector which is bent out of the plane of the imidazole ring by *ca.* 19°. The molecules group around channels of deuteriotrichloromethane, one solvent molecule is disordered around a centre of inversion located between two of its chlorine atoms, thus giving rise to the 5:6 stoichiometry. A hydrogen bond is observed from D(1) to N(13) with C(1)–N(13′) 3.181(9) Å and C(1)–D(1)–N(13′) 156.0° (′ = 2 − *x*, 1 − *y*, 1 − *z*).

Quantum chemical calculations

In order to compare the strength of the Au···Au and Au···Cl interactions in the two crystal structures, calculations were performed on model PH_3AuCl complexes in addition to **2b**. Individual molecules of the complexes were optimised at the B3LYP and MP2 levels of theory. The optimised geometries were then placed in the same relative conformations as those found in the two crystal structures. Single point calculations at the B3LYP and MP2 levels of theory with two different basis

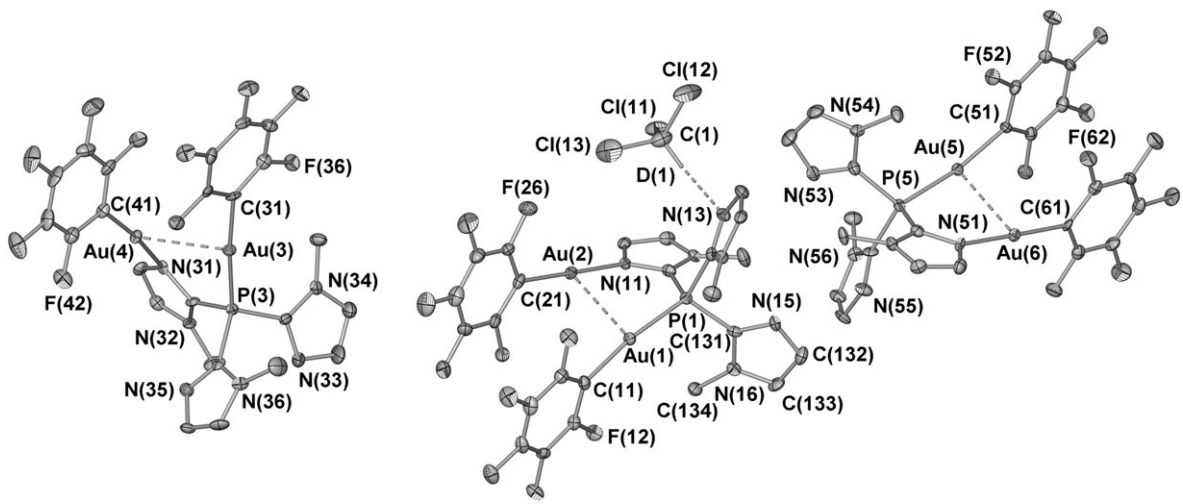

Fig. 9 Molecular structure of compound **4** · $0.83CDCl_3$. Only the deuteriotrichloromethane involved in the hydrogen bond is shown. Thermal ellipsoids are shown at the 50% probability level.

Table 3 Interaction energies[a] of the $(PH_3AuCl)_2$ and $\mathbf{2b}_2$ dimers with Au···Au and Au···Cl interactions, respectively, in kJ mol^{-1}

	PH_3AuCl			$\mathbf{2b}_2$		
	B3LYP/I	B3LYP/II	MP2/II	B3LYP/I	B3LYP/II	MP2/II
Au···Au	−58.1	−45.5	−44.6	−20	−1.6	−0.8
Au···Cl	−36.3	−22.6	−29.9	−22.7	−10.3	−13.1
Δ[b]	21.8	22.9	14.7	−2.6	−8.7	−12.2

[a] Calculated as $E_{dimer} - 2E_{monomer}$. [b] Calculated as $E_{Au\cdots Cl} - E_{Au\cdots Au}$.

sets yielded the interaction energies of the Au···Au and Au···Cl interactions (Table 3). The result for the Au···Au PH_3AuCl interaction energy agrees with that of Pyykkö *et al.*,[43] who found an interaction energy of −24.7 kJ mol^{-1} (−0.009407 Hartree) at the MP2 level, but with a slightly different basis set (see computational details). Table 3 shows that Au···Au interactions between the model PH_3AuCl molecules stabilise the dimers between 14.7 and 22.9 kJ mol^{-1} more than Au···Cl interactions, depending on the level of theory and basis set. This would mean that for a mixture containing $(PH_3AuCl)_2$ dimers, less than 1% would be undergoing Au···Cl interactions.

However, in the case of **2b** the Au···Au interaction is weaker than that of the Au···Cl interaction, resulting in a greater stabilisation of the dimer containing Au···Cl interactions. The differences in interaction energies would mean that a significant portion (>70%) of $\mathbf{2b}_2$ dimers would be stabilised through Au···Cl interactions. Nevertheless, although the Au···Au and Au···Cl interactions play a significant role in stabilising the crystal structures other intermolecular interactions are also involved in the crystal packing, and the influence of these interactions cannot be ruled out as a cause for the relative conformations in the crystal structures.

Conclusions

Several Au^I complexes were structurally characterised and it was shown that the tris(thiazolyl)phosphine ligands are reluctant to coordinate additional Au^I moieties. However, a binuclear complex was obtained with ligand **1a**. The complexes of ligands **1b** and **1c** exhibit markedly different association modes by forming Au···Au or Au···Cl interactions in the solid state, or showing no close interaction with neighbouring molecules depending on the polymorph or cocrystallised solvent. Tris(azolyl)phosphines were shown to be prone to hydrolysis of one azolyl moiety, a property that is currently under investigation in our laboratory.

Experimental

General procedures and instruments

Solvents were dried according to standard procedures and freshly distilled under an atmosphere of dinitrogen.[44] Lithium phenylmethanethiolate, lithium benzenethiolate and lithium thiobenzoate were prepared by treatment of the respective free thiol with butyllithium solution in thf or ether and isolated as solids. Sodium dicyanomethanide was prepared from propanedinitrile and sodium methoxide in methanol. Tris(1-methylimidazol-2-yl)phosphine, tris(thiazol-2-yl)phosphine,[4a] (tht)AuCl[45] and $C_6F_5Au(tht)$[45b] were prepared according to described procedures; ^{13}C NMR data of the ligands were not determined previously and are thus reported here. Melting points were determined with a Stuart Scientific SMP3 apparatus and are uncorrected. Elemental analyses and FAB mass spectra (nitrobenzyl alcohol matrices) were performed by the University of the Witwatersrand. NMR spectra were recorded at the indicated frequency on a Varian VXR 300, Varian Unity INOVA 400 or Varian Unity INOVA 600 instrument at 25 °C. ^1H and ^{13}C NMR spectra were referenced with residual solvent peaks, ^{15}N NMR spectra were referenced externally to neat $MeNO_2$ and ^{31}P NMR spectra were referenced externally to 85% H_3PO_4. EI mass spectra were recorded on an AMD 604 instrument at 70 eV.

Tris(1-methylimidazol-2-yl)phosphine (1a)

δ_H (300 MHz, CD_2Cl_2) 7.11 (6 H, m, H4 + H5) and 3.53 (9 H, s, Me). δ_C (75 MHz, CD_2Cl_2) 141.4 (d, $^1J_{PC}$ 12.0, C2), 130.9 (d, $^3J_{PC}$ 12.0, C4), 130.9 (d, $^3J_{PC}$ 9.1, C4), 130.8 (d, $^3J_{PC}$ 8.9, C4), 125.6–125.5 (3 s, C5) and 34.3 (m, Me). δ_N [61 MHz, $(CD_3)_2SO$] −97.5 (d, $^2J_{PN}$ 50 ± 5, N3) and −208.1 (s, N1). δ_P (121 MHz, CD_2Cl_2) −58.6 (s).

Tris(thiazol-2-yl)phosphine (1b)

δ_H (300 MHz, $CDCl_3$) 8.12 (3 H, d, $^3J_{HH}$ 3.22, H4) and 7.64 (3 H, d, $^3J_{HH}$ 3.22, H5). δ_C (75 MHz, $CDCl_3$) 165.4 (d, $^1J_{PC}$ 14.9, C2), 145.6 (d, $^3J_{PC}$ 11.1, C4) and 124.9 (s, C5). δ_N (61 MHz, CD_2Cl_2) −41.3 (s). δ_P (121 MHz, $CDCl_3$) −31.3 (s).

Tris(4-methylthiazol-2-yl)phosphine (1c)

The ligand was prepared following literature protocol from 4-methylthiazole (3.3 g, 33 mmol) yielding colourless crystals (0.75 g, 28%). In a repeated preparation employing 1.5 g (15 mmol) of 4-methylthiazole, extraction of the aqueous phase with dichloromethane instead of diethyl ether and two crystallisations afforded the product in higher yield (1.27 g, 77%); mp 151 °C. Found: C, 44.15; H, 3.4; N, 12.7. $C_{12}H_{12}N_3PS_3$ requires C, 44.3; H, 3.7; N, 12.9%. δ_H (300 MHz, $CDCl_3$) 7.20 (3 H, qd, $^4J_{HH}$ 0.93, $^4J_{PH}$ 0.49, H5) and 2.48 (9 H, d, $^4J_{HH}$ 0.93, Me). δ_C (75 MHz, $CDCl_3$) 165.4 (d, $^1J_{PC}$ 11.8 Hz, C2), 156.9 (d, $^3J_{PC}$ 13.2, C4), 120.0 (s, C5) and 16.9 (s, Me). δ_N (61 MHz, CD_2Cl_2) −35.4 (s). δ_P (121 MHz, $CDCl_3$) −31.0 (s). *m*/*z* (EI) 325 (24%, M^+) and 227 [100, $(M - C_4H_4NS)^+$].

Tris(4,5-dimethylthiazol-2-yl)phosphine (1d)

In a preparation similar to **1b**, an ethereal solution of 4,5-dimethylthiazole (1.60 cm^3, 15.1 mmol) was added to an ethereal solution of butyllithium (10.0 cm^3 1.51 M in hexanes) cooled to −78 °C. Addition of PCl_3 (0.40 cm^3, 4.6 mmol) dissolved in ether and workup afforded a yellow powder which was triturated with hexane to remove excess dimethylthiazole. Precipitation of the product with hexane from a dichloromethane solution and storage of the suspension overnight yielded well defined crystals amongst the amorphous precipitate (0.30 g, 18%); mp 99 °C. Found: C, 49.2; H, 4.7; N, 11.3. $C_{15}H_{18}N_3PS_3$ requires C, 49.0; H, 4.9; N, 11.4%. δ_H

(300 MHz, CD_2Cl_2) 2.35 (s). δ_C (75 MHz, CD_2Cl_2) 161.3 (d, $^3J_{PC}$ 9.7, C2), 152.7 (d, $^1J_{PC}$ 12.9, C4), 133.7 (s, C5), 14.7 (s, Me) and 11.4 (s, Me). δ_P (121 MHz, CD_2Cl_2) −33.2 (s). *m*/*z* (EI) 383 [15%, $([M + O)^+]$, 367 (30, M^+), 255 [100, $(M - C_5H_6NS)^+$] and 224 [25, $(C_5H_6NS)_2^+$].

Chloro[tris(1-methylimidazol-2-yl)phosphine]gold(I) (2a)

A solution of (tht)AuCl (0.20 g, 0.63 mmol) in dichloromethane (15 cm^3) was reacted with a solution of **1a** (0.17 g, 0.63 mmol) in dichloromethane (10 cm^3). The mixture was stirred overnight and reduced to dryness. The residue was extracted with dichloromethane, filtered through $MgSO_4$ yielding a white solid upon removal of the solvent. Crystallisation from MeOH/thf (5 : 1) layered with diethyl ether at −20 °C afforded a colourless microcrystalline product (0.28 g, 89%). Crystals suitable for X-ray diffraction were grown from a dichloromethane solution layered with diethyl ether; mp 155 (decomp.). Found: C, 28.1; H, 2.9; N, 15.7. $C_{12}H_{15}AuClN_6P \cdot 0.2CH_2Cl_2$ requires C, 28.0; H, 3.0; N, 16.05. δ_H [300 MHz, $(CD_3)_2SO$] 7.71 (3 H, m, H5), 7.26 (3 H, m, H4) and 3.67 (9 H, s, Me). δ_C [75 MHz, $(CD_3)_2SO$] 132.4 (d, $^1J_{PC}$ 121.1, C2), 131.2 (d, $^3J_{PC}$ 17.8, C4), 131.1 (d, $^3J_{PC}$ 17.6, C4), 131.1 (d, $^3J_{PC}$ 17.9, C4), 129.0 (m, C5) and 34.5 (m, Me). δ_N [61 MHz, $(CD_3)_2SO$] −90.6 (d, $^2J_{PN}$ 89.3, N3) and −206.31 (s, N1). δ_P [121 MHz, $(CD_3)_2SO$] −18.4 (s). *m*/*z* (EI) 506 (9%, M^+), 274 [100, $(M - AuCl)^+$], 259 [7, $(M - AuCl - Me)^+$], 193 [44, $(M - AuCl - C_4H_5N_2)^+$] and 112 [30, $(M - AuCl - 2C_4H_5N_2)^+$].

Chloro[tris(thiazol-2-yl)phosphine]gold(I) (2b)

A solution of **1b** (0.12 g, 0.43 mmol) in dichloromethane (5 cm^3) was added to a solution of (tht)AuCl (0.12 g, 0.39 mmol) in dichloromethane (5 cm^3). After stirring for 1 h, $MgSO_4$ was added, the solution was filtered through Celite and the filtrate was concentrated *in vacuo* yielding a white solid. Layering a dichloromethane solution with diethyl ether and storage at −20 °C furnished the compound as colourless crystals (0.18 g, 90%); mp 131 °C (decomp.). Found: C, 21.2; H, 1.2; N, 8.3. $C_9H_6AuClN_3PS_3$ requires C, 21.0; H, 1.2; N, 8.15%. δ_H (300 MHz, CD_2Cl_2) 8.28 (3 H, d, $^3J_{HH}$ 3.03, H4) and 7.91 (3 H, dd, $^3J_{HH}$ 3.03, $^4J_{PH}$ 2.43, H5). δ_C (75 MHz, CD_2Cl_2) 156.8 (d, $^1J_{PC}$ 97.6, C2), 147.6 (d, $^3J_{PC}$ 22.8, C4) and 128.3 (s, C5). δ_N (61 MHz, CD_2Cl_2) −33.9 (d, $^2J_{PN}$ 27.8). δ_P (121 MHz, CD_2Cl_2) 0.9 (s). *m*/*z* (EI) 515 (9%, M^+), 283 [13, $(M - AuCl)^+$] and 199 [100, $(M - AuCl - C_3H_2NS)$].

Chloro[tris(4-methylthiazol-2-yl)phosphine]gold(I) (2c)

In a preparation analogous to **2b**, a solution of (tht)AuCl (0.11 g, 0.35 mmol) in dichloromethane (7.5 cm^3) was added to a solution of **1c** (0.13 g, 0.40 mmol) in dichloromethane (10 cm^3). Recrystallisation afforded colourless crystals (0.18 g, 93%); mp 121 °C (decomp.). Found C, 25.8; H, 2.3; N, 7.7. $C_{12}H_{12}AuClN_3PS_3$ requires C 25.8, H 2.2, N 7.5%. δ_H (300 MHz, CD_2Cl_2) 7.43 (3 H, dq, $^4J_{PH}$ 2.30, $^4J_{HH}$ 0.90, H5) and 2.55 (9 H, dd, $^4J_{HH}$ 0.90, $^5J_{PH}$ 0.50, Me). δ_C (75 MHz, CD_2Cl_2) 155.6 (d, $^1J_{PC}$ 97.5, C2), 158.5 (d, $^3J_{PC}$ 22.1, C4), 123.0 (s, C5) and 17.1 (s, Me). δ_N (61 MHz, CD_2Cl_2) −29.5 (d, $^2J_{PN}$ 89.4). δ_P (121 MHz, CD_2Cl_2) 0.9 (s). *m*/*z* (EI) 557 (3%, M^+), 325 [30, $(M - AuCl)^+$] and 227 [100, $(M - AuCl - C_4H_4NS)^+$].

Chloro[tris(4,5-dimethylthiazol-2-yl)phosphine]gold(I) (2d)

Solid (tht)AuCl (0.30 g, 0.94 mmol) was added to a solution of **1d** (0.35 g, 0.95 mmol) in dichloromethane (20 cm^3). After 1 h the clear solution was filtered through Celite, the filter was washed with dichloromethane (20 cm^3) and the filtrate reduced to dryness. The residue was dissolved in dichloromethane, layered with hexane and stored at −16 °C for 2 days. The mother-liquor was removed and the greenish solid was again dissolved in dichloromethane, the solution was filtered over Celite and the filtrate reduced to dryness yielding yellowish crystals suitable for X-ray diffraction (0.39 g, 67%); mp 86 °C (decomp.). Found: C, 30.2; H, 2.8; N, 6.8. $C_{15}H_{18}AuClN_3PS_3$ requires C, 30.0; H, 3.0; N, 7.0%. δ_H (300 MHz, CD_2Cl_2) 2.42 (9 H, s, 4-Me) and 2.40 (9 H, s, 5-Me). δ_C (75 MHz, CD_2Cl_2) 155.42 (d, $^3J_{PC}$ 21.0, C4), 151.7 (d, $^1J_{PC}$ 99.0, C2), 137.6 (s, C5), 14.9 (s, 4-Me) and 11.6 (s, 5-Me). δ_P (121 MHz, CD_2Cl_2) −0.2 (s). *m*/*z* (FAB) 600 (16, M^+) and 564 [27, $(M - Cl)^+$].

(Thiocyanato)[tris(4-methylthiazolyl)phosphine]gold(I) (3a)

A solution of **2c** (247 mg, 0.44 mmol) in dichloromethane (10 cm^3) was added *via* a Teflon cannula to a degassed aqueous solution of NaNCS (55 mg, 0.68 mmol, 8 cm^3) containing 58 mg K_2SO_4 and the biphasic mixture was stirred vigorously for 3.5 h. The phases were separated with help of a separating funnel and the aqueous phase was extracted with dichloromethane (3 × 3 cm^3). The combined organic phases were dried with Na_2SO_4, filtered and the filter washed with dichloromethane (3 × 5 cm^3). Removal of the solvent *in vacuo* gave a colourless solid (0.24 g, 92%); mp 105 °C (decomp.). Found: C, 26.7; H, 2.0; N, 9.4. $C_{13}H_{12}AuN_4PS_4$ requires C, 26.9; H, 2.1; N, 9.65%. ν_{max}/cm^{-1} 3067s, 2961w, 2918w, 2130s, 2122vs, 2114vs, 2075w, 1497m, 1437m, 1387s, 1360s, 1287m, 1261w, 1055m, 953s, 859s, 765s, 709m. δ_H (300 MHz, CD_2Cl_2) 7.48 (3 H, s, H5) and 2.54 (9 H, s, Me). δ_C (75 MHz, CD_2Cl_2) 159.0 (d, $^3J_{PC}$ 22.3, C4), 155.6 (d, $^1J_{PC}$ 94.9, C2), 123.6 (s, C5), 117.1 (m, SCN) and 17.0 (m, Me). δ_P (121 MHz, CD_2Cl_2) 5.7 (s). *m*/*z* (FAB) 675 [1%, $(M - SCN + C_7H_7NO_3)^+$], 581 [5, $(M + H)^+$] and 522 [7, $(M - SCN)^+$].

(Thiobenzoato)[tris(4-methylthiazol-2-yl)phosphine]gold(I) (3b)

Lithium thiobenzoate (71 mg, 0.49 mmol) was dissolved in thf (25 cm^3). The mixture was stirred for 1.5 h after the addition of **2c** (245 mg, 0.44 mmol). After removal of the solvent the foamy residue was triturated with pentane and dissolved in dichloromethane (15 cm^3), filtered through Celite and the filter washed with dichloromethane. The solution was concentrated *in vacuo*, layered with pentane and stored at −16 °C yielding a yellowish microcrystalline solid (0.25 g, 86%). Crystals of **3b** · $0.5C_6H_{14}$ suitable for X-ray diffraction were grown from a small sample dissolved in dichloromethane and layered with hexane; mp 72 °C. Found: C, 34.4; H, 2.6; N, 6.6. $C_{19}H_{17}AuN_3OPS_4$ requires C, 34.6; H, 2.6; N, 6.4%. ν_{max}/cm^{-1} 3070s, 2953m, 2918m, 2856m, 1622/1616s, 1594w, 1577m, 1495s, 1439s, 1388s, 1362s, 1288m, 1199vs, 1167s, 1063m, 1045m, 953s, 906vs, 860m, 773s, 757s, 714s, 688vs. δ_H (400 MHz,

CD_2Cl_2) 8.05 (2 H, m, *o*-C_6H_5), 7.48 (1 H, m, *p*-C_6H_5), 7.43 (3 H, d, $^4J_{PH}$ 1.05, H5), 7.37 (2 H, m, *m*-C_6H_5) and 2.56 (9 H, s, Me). δ_C (101 MHz, CD_2Cl_2) 158.4 (d, $^3J_{PC}$ 20.7, C4), 156.5 (d, $^1J_{PC}$ 85.5, C2), 141.5 (s, *i*-C_6H_5), 132.3 (s, *p*-C_6H_5), 128.5 (s, *o*/*m*-C_6H_5), 128.2 (s, *m*/*o*-C_6H_5), 122.8 (s, C5) and 17.2 (s, Me). δ_P (162 MHz, CD_2Cl_2) 4.0 (br s). *m*/*z* (FAB) 660 [7%, $(M + H)^+$] and 522 [4, $(M - C_7H_5OS)^+$].

Reaction of chloro[tris(1-methylimidazol-2-yl)phosphine]gold(I) with (pentafluorophenyl)(tetrahydrothiophene)gold(I)

A solution of **1a** (60 mg, 0.1 mmol) in methanol (10 cm^3) was reacted with a solution of C_6F_5Au(tht) (0.16 g, 0.34 mmol) in diethyl ether (10 cm^3). The solution was stirred for 4 h, filtered through Celite and reduced to dryness affording a yellow luminescent product. Recrystallisation by layering an acetone solution with hexane afforded a mixture of colourless crystals of **4** · Me_2CO and yellow needles of **5**. Crystals of both habits were mounted for X-ray diffraction, yet the structure of **5** could not be refined satisfactorily due to crystal twinning and further analyses were hampered by the presence of the compounds as a mixture, only **4** could be obtained in reasonable purity (see below). **5**: mp 136 °C, δ_P [121 MHz, $(CD_3)_2CO$] 126.4 (s).

Bis(pentafluorophenyl)-μ-[tris(1-methylimidazol-2-yl)phosphine-κ^2-*P*,*N*]digold(I) (4)

C_6F_5Au(tht) (261 mg, 0.58 mmol) and **1a** (79 mg, 0.29 mmol) were dissolved in thf (15 cm^3) and the purplish suspension was stirred for 30 min. All volatiles were removed *in vacuo* and the remaining solids were extracted with thf (25 cm^3) and Schlenk-filtered through Celite. Some decomposition occurred during evaporation thus the solid was redissolved in dichloromethane and filtered through Celite. The raw product was recrystallised from acetone layered with pentane and dried *in vacuo*. Yield 0.17 g (29%) of a colourless powder; mp 174 °C. Found: C, 28.9; H, 1.4; N, 8.2. $C_{24}H_{15}Au_2F_{10}N_6P$ requires C, 28.8; H, 1.5; N, 8.4%. δ_H [400 MHz, $(CD_3)_2CO$] 8.00 (1 H, br s, coord. H5), 7.78 (1 H, br s, coord. H4), 7.65 (2H, br s, H5), 7.27 (2H, br s, H4), 4.09 (6 H, s, NMe) and 3.68 (3 H, s, coord. NMe). δ_C [101 MHz, $(CD_3)_2CO$] 149.5 (dm, $^1J_{FC}$ 228, *o*-C_6F_5), 148.4 (dm, $^1J_{FC}$ 227, *o*-C_6F_5), 138 (m, *m*- and *p*-C_6F_5), 132.9 (d, $^3J_{PC}$ 15.0, coord. C4), 132.6 (d, $^3J_{PC}$ 14.2, C4), 132.5 (d, $^1J_{PC}$ 109.5, C2), 131.5 (s, coord. C5), 129.6 (d, $^3J_{PC}$ 1.7, C5), 37.5 (br s, coord. NMe) and 35.6 (d, $^3J_{PC}$ 3.4, NMe). δ_F [376 MHz, $(CD_3)_2CO$] −115.2 (2 F, m, *o*-C_6F_5), −115.3 (2 F, m, *o*-C_6F_5), −164.0 (2 F, m, *m*-C_6F_5), −164.7 (2 F, m, *m*-C_6F_5), −160.4 (1 F, t, $^3J_{FF}$ 19.3, *p*-C_6F_5) and −162.1 (1 F, t, $^3J_{FF}$ 19.6, *p*-C_6F_5) δ_P [162 MHz, $(CD_3)_2CO$] −2.7 (s). *m*/*z* (FAB) 1003 [15%, $(M + H)^+$], 1002 (7, M^+), 835 [12, $(M - C_6F_5)^+$], 639 [18, $(M - AuC_6F_5 + H)^+$], 471 (8, LAu^+), 275 [30, $(L + H)^+$] and 193 [18, $(L - C_4H_5N_2)^+$].

Crystal structure determinations

Data associated with the crystal structures are summarised in Table 4. Intensity data were collected at T = 100 K with a Bruker SMART Apex diffractometer[46] with graphite monochromated Mo-Kα radiation (λ = 0.71073 Å). Intensities were measured using the ω-scan mode and were corrected for Lorentz and polarisation effects. Intensity data for **2b(i)** were collected at T = 203 K with a Nonius Kappa CCD diffractometer with graphite monochromated Mo-Kα radiation using φ- and ω-scans.[47] The structures were solved by direct methods or the heavy atom(s) were located by a Patterson synthesis and refined by full-matrix least-squares on F^2 using the SHELXL-97 software package within the X-SEED environment.[48] All non-hydrogen atoms were refined with anisotropic displacement parameters except if noted below and all hydrogens were placed in calculated positions. Figures were created using POV-Ray 3.5, hydrogen atoms were omitted for clarity throughout.

While solving the structure of **2d**, the thiazole ring containing C(11) was found to be disordered in two positions related by a 180° rotation and populated 3 : 1; satisfactory modelling of the rings could only be achieved by splitting S(11) and N(11), thus giving average positions of the two orientations for the carbons in the thiazole ring, and constraining the rings to be flat. The anisotropic displacement parameters of S(11) and N(11), respectively, were constrained to be equal. It is also possible to solve the crystal structure of **2b** in space group *Pnma* but this imposes the same disorder on the other thiazole rings which have a defined orientation in space group $Pna2_1$. After establishing the connectivity of **3b**, additional diffuse electron density which belongs to cocrystallised hexane solvent was located on the difference map, but could not be modelled. It was removed using the Squeeze routine in the Platon programme package.[49] The phenyl ring of the thiobenzoate was found to be disordered populating two different orientations in a 3 : 2 ratio which were constrained as flat regular hexagons and only the major orientation refined anisotropically constraining C(42A) and C(43A) to have similar anisotropic displacement parameters. An acetone molecule was located in the difference map of compound **4** but could not be refined anisotropically, the C–C bonds were restrained to 1.48 Å and the C=O bond to 1.22 Å. Due to large U_{iso} values its occupancy factor was allowed to refine freely and found to be 0.77 resulting from loss of solvent during setup of the crystal.

CCDC reference numbers 659052–659064.

For crystallographic data in CIF or other electronic format see DOI: 10.1039/b709896k

Computational methods

The geometry of PH_3AuCl was optimised at the gradient-corrected DFT level using the three parameter fit of the exchange–correlation potential suggested by Becke[50] in conjunction with the LYP[51] exchange potential (B3LYP).[52] A quasi-relativistic small-core ECP with a (341/321/21)[53] valence basis set for the gold atom and the 6-311 + G(d) all-electron basis set[54] (basis set I) for the other atoms were employed in the geometry optimisation. The nature of the stationary point was examined by calculating the Hessian matrix at this level: the structure is an energy minima on the potential energy surface. The optimised structure was placed in the same relative conformations as the experimental crystal structures. Single point calculations were performed using B3LYP, and by including electron correlation at the second-order

Table 4 Crystallographic and data collection parameters

Compound	**1d**	**2a**	**2b(i)**	**2b(ii)**	**2b(iii)**	**2b** · $0.5CH_2Cl_2$	**2c(i)**	**2c(ii)**	**2c** · thf[b]	**2d**[c]	**3b** · $0.5C_6H_{14}$	**4** · Me_2CO	**4** · $0.83CDCl_3$
Empirical formula	$C_{15}H_{18}N_3PS_3$	$C_{12}H_{15}AuClN_6P$	$C_9H_6AuClN_3PS_3$	$C_9H_6AuClN_3PS_3$	$C_9H_6AuClN_3PS_3$	$C_{9.5}H_7AuCl_2N_3PS_3$	$C_{12}H_{12}AuClN_3PS_3$	$C_{12}H_{12}AuClN_3PS_3$	$C_{16}H_{20}AuClN_3OPS_3$	$C_{15}H_{18}AuClN_3PS_3$	$C_{22}H_{24}AuN_3OPS_4$	$C_{27}H_{21}Au_2F_{10}N_6OP$	$C_{24.83}H_{15}Au_2Cl_{2.5}D_{0.83}F_{10}N_6P$
M_r	367.49	506.68	515.75	515.75	515.73	558.22	557.83	557.83	629.94	599.91	702.62	1060.4	1103
Crystal habit	Prism	Prism	Block	Block	Block	Needle	Block	Needle	Prism	Block	Block	Plate	Prism
Crystal size/mm	0.10 × 0.03 × 0.03	0.31 × 0.10 × 0.07	0.15 × 0.07 × 0.05	0.20 × 0.15 × 0.10	0.33 × 0.15 × 0.14	0.34 × 0.08 × 0.05	0.20 × 0.20 × 0.10	0.96 × 0.28 × 0.21	0.04 × 0.03 × 0.01	0.05 × 0.03 × 0.01	0.03 × 0.01 × 0.01	0.15 × 0.15 × 0.05	0.24 × 0.13 × 0.11
Crystal system	Monoclinic	Monoclinic	Monoclinic	Triclinic	Triclinic	Monoclinic	Monoclinic	Monoclinic	Orthorhombic	Orthorhombic	Orthorhombic	Triclinic	Triclinic
Space group	$P2_1/n$	$P2_1/n$	$P2_1/c$	$P\bar{1}$	$P\bar{1}$	$P2_1/n$	$C2/c$	$P2_1/c$	$P2_12_12_1$	$Pna2_1$	$Pbca$	$P\bar{1}$	$P\bar{1}$
a/Å	12.760(1)	7.765(2)	10.3829(1)	8.0705(4)	8.611(2)	7.9518(9)	23.574(2)	19.822(2)	9.0405(9)	12.954(2)	10.6209(8)	10.280(2)	12.325(1)
b/Å	9.7885(9)	18.867(5)	16.2935(1)	8.6077(4)	8.701(2)	20.261(2)	10.7660(9)	10.333(1)	9.653(1)	11.294(1)	17.664(1)	12.707(2)	19.123(2)
c/Å	13.923(1)	11.069(3)	17.2073(2)	10.5184(5)	9.512(2)	19.413(2)	17.201(2)	17.544(2)	24.273(3)	13.366(2)	27.839(2)	13.141(2)	20.242(2)
α/°	90	90	90	72.425(1)	90.821(3)	90	90	90	90	90	90	81.504(2)	101.251(2)
β/°	101.800(2)	90.540(4)	92.3216(4)	84.882(1)	97.446(3)	96.018(2)	128.280(1)	109.950(1)	90	90	90	81.244(3)	98.052(2)
γ/°	90	90	90	75.129(1)	106.515(3)	90	90	90	90	90	90	72.231(2)	100.106(2)
V/Å^3	1702.3(3)	1621.6(7)	2908.63(5)	673.20(6)	676.5(2)	3110.6(6)	3426.9(5)	3377.7(6)	2118.3(4)	1955.6(4)	5222.7(7)	1606.3(4)	4530.7(8)
Z, D_c/Mg m^{-3}	4, 1.434	4, 2.075	8, 2.355	2, 2.544	2, 2.532	8, 2.384	8, 2.162	8, 2.194	4, 1.975	4, 2.038	8, 1,787	2, 2.165[d]	6, 2.425
μ(Mo-Kα)/mm^{-1}	0.528	9.337	10.823	11.690	11.634	10.296	9.195	9.329	7.454	8.064	6.035	9.262[d]	10.069
No. of reflections	9941	8961	21 538	7454	7937	17 633	9974	35 125	12 563	11 189	29 548	9403	47 479
Unique	3606	3253	5711	2842	3162	6344	3639	6921	4472	3661	5534	6595	18211
R_{int}	0.0206	0.0269	0.0250	0.251	0.0281	0.0675	0.0222	0.0409	0.0326	0.0261	0.0393	0.0262	0.0334
hkl index range	−16 to 14, ±12, −15 to 17	± 9, −22 to 23, −13 to 8	±12, ±20, ±21	±10, ±10, ±13	±11, ±11, ±12	±9, −25 to 17, −22 to 24	±29, −7 to 13, ±21	±24, ±12, ±21	−11 to 7, −12 to 10, ±30	−16 to 15, −10 to 14, −16 to 14	−10 to 13, −20 to 22, −34 to 35	−12 to 13, −15 to 16, −16 to 10	±15, ±23, ±25
Data, restraints, params.	3327, 0, 205	2740, 8, 215	5042, 0, 325	2744, 0, 163	3073, 0, 163	4748, 0, 352	3390, 0, 193	6630, 0, 385	4210, 0, 238	3469, 9, 236	4937, 12, 266	5084, 2, 408	14 419, 0, 1270
F(000)	768	960	1920	480	480	2088	2112	2112	1216	1152	2744	977.3[d]	3074
$R1$, wR_2[a] [$I > 2\sigma(I)$]	0.0296, 0.0766	0.0308, 0.0657	0.0207, 0.0422	0.0192, 0.0449	0.0187, 0.0439	0.0481, 0.0833	0.0204, 0.0473	0.0263, 0.0620	0.0245, 0.0489	0.0237, 0.0581	0.0470, 0.1051	0.0447, 0.1043	0.0288, 0.0450
R_1, wR_2 (all data)	0.0320, 0.0783	0.0412, 0.0699	0.0272, 0.0439	0.0202, 0.0453	0.0195, 0.0442	0.0739, 0.0909	0.0225, 0.0482	0.0277, 0.0626	0.0268, 0.0495	0.0255, 0.0591	0.0531, 0.1075	0.0635, 0.1130	0.0622, 0.0761
Goodness-of-fit	1.076	1.041	1.033	1.028	1.054	0.991	1.058	1.170	0.906	1.048	1.206	0.997	1.083

[a] $w = 1/[\sigma^2(F_o)^2 + aP^2 + bP]$ where $P = (F_o^2 + 2F_c^2)/3$. [b] Flack x parameter 0.015(5). [c] Flack x parameter 0.519(7). [d] Values for acetone occupancy of 0.77.

Møller–Plesset (MP2) level. The calculations were repeated using the 19 valence-electron (VE) quasi-relativistic (QR) pseudopotentials of Andrae *et al.*[55] for Au, with the addition of two f-type polarisation functions for a more accurate description of the interaction energy,[43] and the 6-311 + G(d) all-electron basis set[54] (basis set II) for the other atoms. The calculations were performed with a parallel version of the programme package Gaussian 03.[56]

Acknowledgements

We would like to thank Stellenbosch University and Harmony Gold for financial support and Mintek project Autek for the generous loan of gold.

References

1 (*a*) A. Burini, B. R. Pietroni, R. Galassi, G. Valle and S. Calogero, *Inorg. Chim. Acta*, 1995, **229**, 299–305; (*b*) F. Bachechi, A. Burini, M. Fontani, R. Galassi, A. Macchioni, B. R. Pietroni, P. Zanello and C. Zuccaccia, *Inorg. Chim. Acta*, 2001, **323**, 45–54.
2 V. J. Catalano and S. J. Horner, *Inorg. Chem.*, 2003, **42**, 8430–8438.
3 (*a*) P. C. Kunz, G. J. Reiß, W. Frank and W. Kläui, *Eur. J. Inorg. Chem.*, 2003, 3945–3951; (*b*) C. Kimblin, B. M. Bridgewater, D. G. Churchill and G. Parkin, *J. Chem. Soc., Dalton Trans.*, 2000, 2191–2194; (*c*) T. B. Koerner and R. S. Brown, *Can. J. Chem.*, 2002, **80**, 183–191.
4 (*a*) S. S. Moore and G. M. Whitesides, *J. Org. Chem.*, 1982, **47**, 1489–1493; (*b*) R. A. Bell, C. J. L. Lock, C. Scholten and J. F. Valliant, *Inorg. Chim. Acta*, 1998, **274**, 137–142.
5 A. Antiñolo, F. Carrillo-Hermosilla, E. Díez-Barra, J. Fernández-Baeza, A. Lara-Sánchez, A. Otero and J. Tejeda, *J. Organomet. Chem.*, 1998, **570**, 97–105.
6 E. J. Fernández, A. Laguna, J. M. López-de-Luzuriaga, M. Monge, M. Montiel, M. E. Olmos and M. Rodríguez-Castillo, *Dalton Trans.*, 2006, 3672–3677.
7 M. F. M. Al-Dulaymmi, A. Hills, P. B. Hitchcock, D. L. Hughes and R. L. Richards, *J. Chem. Soc., Dalton Trans.*, 1992, 241–248.
8 S.-M. Kuang, Z.-Z. Zhang, F. Xue and T. C. W. Mak, *J. Organomet. Chem.*, 1999, **575**, 51–56.
9 A. Neveling, G. R. Julius, S. Cronje, C. Esterhuysen and H. G. Raubenheimer, *Dalton Trans.*, 2005, 181–192.
10 D. Carmona, C. Vega, N. García, F. J. Lahoz, S. Elipe, L. A. Oro, M. P. Lamata, F. Viguri and R. Borao, *Organometallics*, 2006, **25**, 1592–1606.
11 D. Schneider, S. Nogai, A. Schier and H. Schmidbaur, *Inorg. Chim. Acta*, 2003, **352**, 179–187.
12 M. Nakamoto, W. Hiller and H. Schmidbaur, *Chem. Ber.*, 1993, **126**, 605–610.
13 K. Nunokawa, S. Onaka, T. Tatematsu, M. Ito and J. Sakai, *Inorg. Chim. Acta*, 2001, **322**, 56–64.
14 (*a*) D. W. Allen, B. G. Hutley and M. T. J. Mellor, *J. Chem. Soc., Perkin Trans. 2*, 1972, 63–67; (*b*) D. W. Allen, B. G. Hutley and M. T. J. Mellor, *J. Chem. Soc., Perkin Trans. 2*, 1977, 1705–1708.
15 J. F. Britten, C. J. L. Lock and Z. Wang, *Acta Crystallogr., Sect. C: Cryst. Struct. Commun.*, 1992, **48**, 1600–1603.
16 D. Copping, C. S. Frampton, H. E. Howard-Lock and C. J. L. Lock, *Acta Crystallogr., Sect. C: Cryst. Struct. Commun.*, 1992, **48**, 675–677.
17 C. Kimblin, V. J. Murphy, T. Hascall, B. M. Bridgewater, J. B. Bonanno and G. Parkin, *Inorg. Chem.*, 2000, **39**, 967–974.
18 (*a*) W. Kläui, C. Piefer, G. Rheinwald and H. Lang, *Eur. J. Inorg. Chem.*, 2000, 1549–1555; (*b*) A. Schiller, R. Scopelliti, M. Benmelouka and K. Severin, *Inorg. Chem.*, 2005, **44**, 6482–6492.
19 (*a*) T. N. Sorrell, W. E. Allen and P. S. White, *Inorg. Chem.*, 1995, **34**, 952–960; (*b*) M. Enders, O. Fritz and H. Pritzkow, *Z. Anorg. Allg. Chem.*, 2004, **630**, 1501–1506.
20 G. H. Woehrle, L. O. Brown and J. E. Hutchison, *J. Am. Chem. Soc.*, 2005, **127**, 2172–2183.
21 G. A. Gray and T. A. Albright, *J. Am. Chem. Soc.*, 1976, **98**, 3857–3861.
22 (*a*) H. V. R. Dias and W. Jin, *Inorg. Chem.*, 1996, **35**, 3687–3694; (*b*) G. Gioia Lobbia, J. V. Hanna, M. Pellei, C. Pettinari, C. Santini, B. W. Skelton and A. H. White, *Dalton Trans.*, 2004, 951–958.
23 S. Cronje, H. G. Raubenheimer, H. S. C. Spies, C. Esterhuysen, H. Schmidbaur, A. Schier and G. J. Kruger, *Dalton Trans.*, 2003, 2859–2866.
24 (*a*) B. Wrackmeyer, G. Kehr and H. Zhou, *Fresenius' J. Anal. Chem.*, 1998, **357**, 489–493; (*b*) R. Schmutzler, P. Bernatowicz, W. Schilf, L. Stefaniak and G. A. Webb, *J. Mol. Struct.*, 1997, **442**, 121–123; (*c*) J. Peralta-Cruz, V. I. Bakhmutov and A. Ariza-Castolo, *Magn. Reson. Chem.*, 2001, **39**, 187–193.
25 B. C. Chen, W. von Philipsborn and K. Nagarajan, *Helv. Chim. Acta*, 1983, **66**, 1537–1555.
26 J. P. Warren and J. D. Roberts, *J. Phys. Chem.*, 1974, **78**, 2507–2511.
27 A. L. Balch, *Gold Bull.*, 2004, **37**, 45–50.
28 (*a*) P. Schwerdtfeger, H. L. Hermann and H. Schmidbaur, *Inorg. Chem.*, 2003, **42**, 1334–1342; (*b*) E. O'Grady and N. Kaltsoyannis, *Phys. Chem. Chem. Phys.*, 2004, **6**, 680–687.
29 S. Y. Ho and E. R. T. Tiekink, *Z. Kristallogr.–New Cryst. Struct.*, 2002, **217**, 591–592.
30 U. Monkowius, S. Nogai and H. Schmidbaur, *Z. Naturforsch., B: Chem. Sci.*, 2003, **58**, 751–758.
31 (*a*) H. W. Chen and E. R. T. Tiekink, *Acta Crystallogr., Sect. E: Struct. Rep. Online*, 2003, **59**, m50–m51; (*b*) P. Tasker, D. Coventry, S. Parsons and D. Messenger, personal communication to Cambridge Crystallographic Data Centre, 2005, CCDC No. 276800.
32 (*a*) Z. Assefa, B. G. McBurnett, R. J. Staples, J. P. Fackler, Jr, B. Assmann, K. Angermaier and H. Schmidbaur, *Inorg. Chem.*, 1995, **34**, 75–83; (*b*) Z. Assefa, M. A. Omary, B. G. McBurnett, A. A. Mohamed, H. H. Patterson, R. J. Staples and J. P. Fackler, Jr., *Inorg. Chem.*, 2002, **41**, 6274–6280.
33 F. Jiang, M. M. Olmstead and A.L. Balch, *J. Chem. Soc., Dalton Trans.*, 2000, 4098–4103.
34 A. Codina, E. J. Fernández, P. G. Jones, A. Laguna, J. M. López-de-Luzuriaga, M. Monge, M. E. Olmos, J. Pérez and M. A. Rodriguez, *J. Am. Chem. Soc.*, 2002, **124**, 6781–6786.
35 (*a*) P. D. Cookson and E. R. T. Tiekink, *Acta Crystallogr., Sect. C: Cryst. Struct. Commun.*, 1994, **50**, 1896–1898; (*b*) R. C. Bott, P. C. Healy and G. Smith, *Aust. J. Chem.*, 2004, **57**, 213–218.
36 (*a*) H. Schmidbaur, A. Wohlleben, F. Wagner, O. Orama and G. Huttner, *Chem. Ber.*, 1977, **110**, 1748–1754; (*b*) P. C. Healy, *Acta Crystallogr. Sect. E: Struct. Rep. Online*, 2003, **59**, m1112–m1114.
37 J. Bernstein, R. J. Davey and J.-O. Henck, *Angew. Chem., Int. Ed.*, 1999, **38**, 3440–3461.
38 M. Preisenberger, A. Schier and H. Schmidbaur, *Z. Naturforsch., B: Chem. Sci.*, 1998, **53**, 781–787.
39 (*a*) A. Kolb, P. Bissinger and H. Schmidbaur, *Z. Anorg. Allg. Chem.*, 1993, **619**, 1580–1588; (*b*) Y. Yang, V. Ramamoorthy and P. R. Sharp, *Inorg. Chem.*, 1993, **32**, 1946–1950.
40 P. G. Jones and C. Thöne, *Acta Crystallogr., Sect. C: Cryst. Struct. Commun.*, 1992, **48**, 1312–1314.
41 N. C. Baenziger, W. E. Bennett and D. M. Soboroff, *Acta Crystallogr., Sect. B: Struct. Crystallogr. Struct. Chem.*, 1976, **32**, 962–963.
42 R. W. Baker and P. J. Pauling, *J. Chem. Soc., Dalton Trans.*, 1972, 2264–2266.
43 P. Pyykkö, N. Runeberg and F. Mendizabal, *Chem. Eur. J.*, 1997, **3**, 1451–1457.
44 R. J. Errington, in *Advanced Practical Inorganic and Metalorganic Chemistry*, Chapman & Hall, London, 1997, p. 92.
45 (*a*) A. Haas, J. Helmbrecht and U. Niemann, in *Handbuch der Präparativen Anorganischen Chemie*, ed. G. Brauer, Stuttgart, Enke, 1978, p. 1014; (*b*) R. Uson, A. Laguna and M. Laguna, *Inorg. Synth.*, 1989, **26**, 85–91.
46 (*a*) SMART Data collection software (v 5.629), Bruker AXS Inc., Madison WI, 2003; (*b*) SAINT Data reduction software (v 6.45), Bruker AXS Inc., Madison WI, 2003; (*c*) R. H. Blessing, *Acta*

Crystallogr., Sect. A: Fundam. Crystallogr., 1995, **51**, 33–38; (*d*) SADABS Absorption correction software (v. 2.05), Bruker AXS Inc., Madison WI, 2002.
47 (*a*) COLLECT, Data collection software, Nonius BV, Delft, The Netherlands, 1998; (*b*) DENZO, Program for data reduction, Z. Otwinowski and W. Minor, *Methods Enzymol.*, 1997, **276**, 307–326.
48 (*a*) G. M. Sheldrick, *SHELX97, Programmes for crystal structure solution and refinement*, University of Göttingen, Germany, 1997; (*b*) L. J. Barbour, *J. Supramol. Chem.*, 2001, **1**, 189–191; (*c*) J. L. Atwood and L. J. Barbour, *Cryst. Growth Des.*, 2003, **3**, 3–8.
49 A. L. Spek, *J. Appl. Crystallogr.*, 2003, **36**, 7–13.
50 A. D. Becke, *J. Chem. Phys.*, 1993, **98**, 5648–5652.
51 C. Lee, W. Yang and R. G. Parr, *Phys. Rev. B: Condens. Matter*, 1988, **37**, 785–789.
52 P. J. Stephens, F. J. Devlin, C. F. Chabalowski and M. J. Frisch, *J. Phys. Chem.*, 1994, **98**, 11623–11627.
53 P. J. Hay and W. R. Wadt, *J. Chem. Phys.*, 1985, **82**, 299–310.
54 (*a*) R. Ditchfield, W. J. Hehre and J. A. Pople, *J. Chem. Phys.*, 1971, **54**, 724–728; (*b*) W. J. Hehre, R. Ditchfield and J. A. Pople, *J. Chem. Phys.*, 1972, **56**, 2257–2261.
55 D. Andrae, U. Häußermann, M. Dolg, H. Stoll and H. Preuß, *Theor. Chim. Acta*, 1990, **77**, 123–141.
56 M. J. Frisch, G. W. Trucks, H. B. Schlegel, G. E. Scuseria, M. A. Robb, J. R. Cheeseman, V. G. Zakrzewski, J. A. Montgomery, Jr., R. E. Stratmann, J. C. Burant, S. Dapprich, J. M. Millam, A. D. Daniels, K. N. Kudin, M. C. Strain, O. Farkas, J. Tomasi, V. Barone, M. Cossi, R. Cammi, B. Mennucci, C. Pomelli, C. Adamo, S. Clifford, J. Ochterski, G. A. Petersson, P. Y. Ayala, Q. Cui, K. Morokuma, D. K. Malick, A. D. Rabuck, K. Raghavachari, J. B. Foresman, J. Cioslowski, J. V. Ortiz, A. G. Baboul, B. B. Stefanov, G. Liu, A. Liashenko, P. Piskorz, I. Komaromi, R. Gomperts, R. L. Martin, D. J. Fox, T. Keith, M. A. Al-Laham, C. Y. Peng, A. Nanayakkara, C. Gonzalez, M. Challacombe, P. M. W. Gill, B. G. Johnson, W. Chen, M. W. Wong, J. L. Andres, M. Head-Gordon, E. S. Replogle and J. A. Pople, *GAUSSIAN 98 (Revision A.8)*, Gaussian, Inc., Pittsburgh, PA, 1998.

